UPGRADING THE COMPRESSOR STAGE OF A SOLARISED MICRO GAS TURBINE

Michael Fivaz[1], Johan van der Spuy[2], and Hano van Eck[3]

[1] Solar Thermal Energy Research Group (STERG), Department of Mechanical and Mechatronic Engineering, Stellenbosch University, Joubert Street, Matieland 7602, Stellenbosch, South Africa; Phone: +27736842438; Email: 21555931@sun.ac.za

[2] Solar Thermal Energy Research Group (STERG), Department of Mechanical and Mechatronic Engineering, Stellenbosch University; Email: sjvdspuy@sun.ac.za

[3] Department of Military Technology, Stellenbosch University; Email: hvaneck@sun.ac.za

Abstract: A solar-hybrid gas turbine combines the environmental advantages of concentrating solar power (CSP) with the capabilities of a micro gas turbine's (MGT) continuous high-power output. A variety of options are available to improve MGT's performance and efficiency, with the primary focus being on its compression stage. An upgraded compressor stage for an existing solar-hybrid application MGT testbench is presented. MGT engines commonly feature a centrifugal compressor stage due to higher per stage pressure ratios being achieved compared to single stage axial configurations. The existing operational solar-hybrid MGT testbench, operates at low efficiency. The impeller of the MGT is redesigned by first simulating the existing impeller in a computational fluid dynamics (CFD) simulation and comparing the results to its existing performance charts. It is then redesigned with a one-dimensional (1D) mean line code and simulated in CFD to evaluate performance improvement. The new design is further improved by increasing the geometrical tolerances of the impeller stage's tip gaps to the finest achievable manufacturing tolerance of 0.3 mm. This improvement increases the simulated pressure ratio and efficiency of the MGT compressor from 1.482 to 1.55 and 78.3% to 84.2%, respectively. The MGT testbench predicted overall output power improves by 22.7%, from 18.078 kW to 22.186 kW. Due to a redesigned impeller and finer impeller clearance tolerance requirements, both the impeller and shroud cover need to be re-manufactured. This enables the centrifugal compressor to provide its optimal performance based on geometrical limitations.

Keywords: Centrifugal compressor design; Micro gas turbine; Solar-hybrid gas turbine.

1. Introduction

South Africa is blessed with some of the highest Direct Normal Irradiance (DNI) levels in the world, with certain regions receiving more than 9 kWh/m^2 each day, equating to 3 287 kWh/m^2 annually according to [1]. These high DNI zones in South Africa, particularly in the Northern Cape, are regarded to be relatively remote, with few human settlements and dry, flat landscapes. As a result, this area is particularly suitable for harnessing the sun's energy for renewable energy generation.

A small-scale concentrating solar power (CSP) system based on the Stellenbosch University Solar Power Thermodynamic (SUNSPOT) cycle (proposed by [2]), has been investigated at Stellenbosch University's Mechanical and Mechatronic Engineering Department. The SUNSPOT cycle integrates a conventional CSP plant with a Brayton cycle gas turbine generator, offering the benefits of a hybrid system. This cycle is represented in Fig. 1 below, where the Brayton cycle is coupled to the CSP plant through the combustor and turbine.

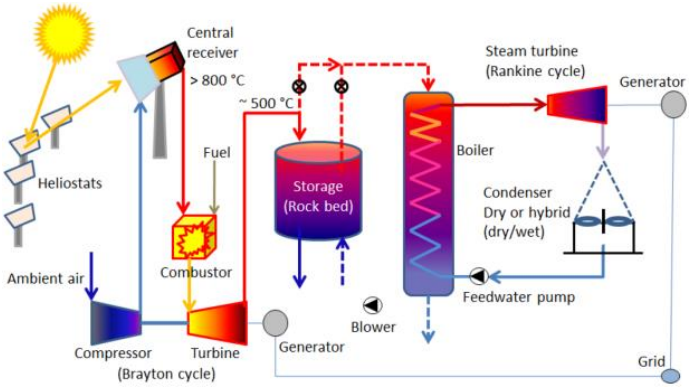

Fig. 1. The SUNSPOT cycle (proposed by [2])

Sunlight is reflected onto a central receiver tower by heliostat mirrors, which transports heat to the gas turbine that generates a significant amount of heat on its own. This heat is then transferred from the gas turbine to a storage facility, where the

remainder of the cycle functions as a traditional CSP plant. That is, steam is produced by a boiler and used to drive a steam turbine, which generates electricity through a generator. The remaining work produced by the gas turbine is transferred to another generator and contributes to overall electricity generation. The performance of the gas turbine generator is therefore essential to the overall efficiency of the SUNSPOT cycle.

The micro gas turbine (MGT) testbench, designed and built by [3] and intended for use in a solar-hybrid application, has a twin-spool and twin-shaft configuration. The gas generator and power turbine sections were developed by using BorgWarner K31 and K44 turbocharger models respectively. The K44 model, which initially served as the power turbine, is replaced by another K31 model that offers a better operating point for the engine. Therefore, both the gas generator and power turbine sections now feature the same K31 model. The tubular style combustion chamber was designed and built by [4] for an MGT engine similarly to the K31 turbocharger setup. This MGT engine is depicted in a flow diagram in Fig. 2 below, with the central receiver system omitted because the focus of this work is on the MGT engine.

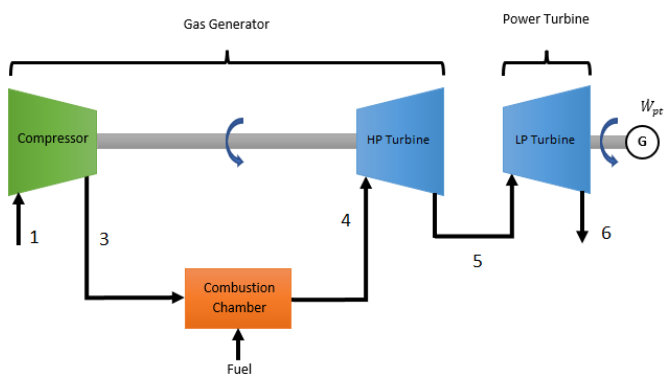

Fig. 2. Layout of twin-shaft MGT system (acquired from [5])

The K31 model, acting as the gas generator, includes the compressor and high pressure (HP) turbine. Whereas the other K31 model, acting as the power turbine, includes the low pressure (LP) turbine and output power section. This K31 model's compressor is omitted since it acts purely as a load for the LP turbine to drive, which will later be replaced with a generator. The inlet and outlet of each stage is labelled, and the compression stage, which is the primary focus of this paper consists of a centrifugal impeller and a diffuser separated by point 2.

According to [6] a centrifugal impeller uses centrifugal force to propel fluid outwards, where the fluid's energy increases through raising static pressure and velocity levels. As it exits the impeller, the diffuser converts kinetic energy into pressure energy.

This paper investigates the effect of upgrading the compression stage of the twin-shaft MGT testbench engine, on overall system performance and operating efficiency. This is accomplished by redesigning the compressor's centrifugal impeller and diffuser using a one dimensional (1D) mean line code. On the new design, a computational fluid dynamic (CFD) simulation is carried out to provide compressor performance charts that allow the performance of the system to be analysed and compared to the existing one. A model of the engine has been developed in a fluid network simulation program by [7], which is used to evaluate the overall improvement of the new compressor design.

Previous research on designing centrifugal compressors focused mostly on acquiring a design methodology and testing the new design on an MGT engine for performance improvement evaluations. This design methodology entails first replicating the original impeller's geometry, then subjecting it to a CFD analysis and comparing the performance results to the original. Subsequently, a new impeller design is optimised using the 1D mean-line code to achieve the desired performance. The improved pressure ratio and efficiency performance charts of the new impeller design, obtained from its CFD analysis, are then tested and compared to those of the replicated design.

2. Flownex® Model

Flownex® (2022b), a fluid network simulation program, is used to model different properties such as mass flow, pressure, and temperature, as well as any other fluid properties required for performance analysis of a system. It solves the mass, momentum, and energy conservation equations to acquire the results. The Flownex® program constructs a network representing a system by using component icons made up of nodes, elements, and boundary conditions. The settings for each of these components can be adjusted to correctly portray the fluid conditions and the engine's size proportion.

2.1. Twin-Shaft MGT Flownex® Model

The twin-shaft micro gas turbine (MGT), developed by [3], was successfully modelled using Flownex® by [7]. This model's nodes, elements, and boundary conditions are presented in Fig. 3. It has been altered from its original layout to be superimposed on the flow diagram in Fig. 2.

The components of the compressor's inlet mimic a bellmouth, with the fluid adjusted to precisely match that of ambient air entering the engine. It is powered by a high pressure (HP) turbine, which is represented by a rotating shaft element, and its outlet is connected to the combustion chamber.

The addition of fuel to the inlet of the combustion chamber

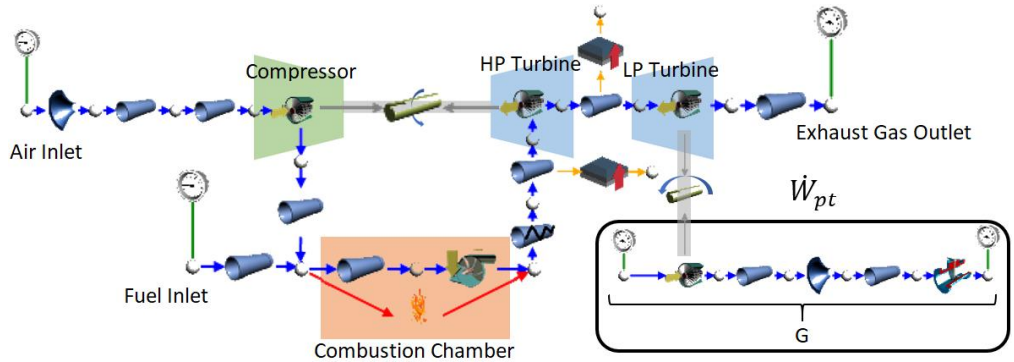

Fig. 3. Flownex® model of twin-shaft MGT (Adapted from [7])

represents an increase in the mass flow rate of fluid going through. To depict the behavior of internal combustion, the combustion chamber is made up of a pipe, a pump, and an adiabatic flame element. The outlet of the combustion chamber is connected to the HP turbine via a resistive network pipe and a heat transfer element which indicates friction and heat loss.

The outlet of the HP turbine is connected to the low pressure (LP) turbine via a heat transfer pipe element, also indicating heat loss. Its outlet is open to the atmosphere, as defined by the boundary condition.

The LP turbine is intended to power a generator that generates electricity; however, this model incorporates a load compressor which the LP turbine drives. This load compressor, which is likewise linked with piping elements, serves as a load for the LP turbine, which is regarded as the overall engine output power.

2.2. Compressor Maps

Compression and efficiency performance charts (compressor maps) portray the relationship between pressure ratio and mass flow rate, with superimposed rotational speed curves and efficiency contours. These compressor maps are what define a specific compressor in Flownex®, where the data is interpolated and any operating points within the compressor range can be predicted. Fig. 4 shows a compressor map labelled with all the essential components.

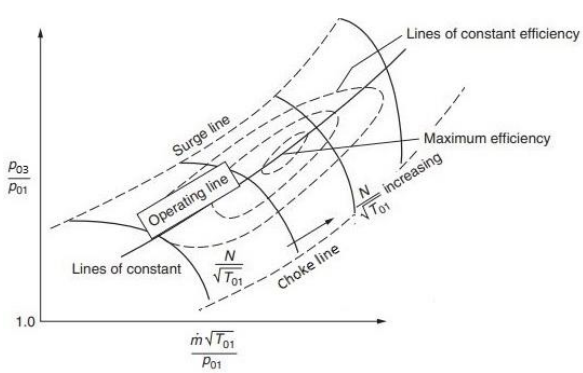

Fig. 4. Compressor map (acquired from [6])

The subscripts 1 and 3 refer to the compressor's inlet and outlet, respectively, with the suffix 0 indicating stagnation (total) conditions. The vertical axis label is the pressure ratio, $\frac{P_{03}}{P_{01}}$, plotted as a function of $\frac{\dot{m}\sqrt{T_{01}}}{P_{01}}$ for fixed values of $\frac{N}{\sqrt{T_{01}}}$. The constant efficiency islands are calculated using Eq. (2), derived in [6] from the pressure ratio (Eq. (1)), where k is the specific heat ratio of air, yielding the ideal running point regions.

$$PR_{C(T-T)} = \left(\frac{P_{03}}{P_{01}}\right) \tag{1}$$

$$\eta_{C(T-T)} = \frac{\left(\frac{P_{03}}{P_{01}}\right)^{\frac{k-1}{k}} - 1}{\left(\frac{T_{03}}{T_{01}}\right) - 1} \tag{2}$$

At the upper pressure ratio, the stall point region is where the constant speed curves end and the compressor becomes unstable. The choke point region is when the constant speed curves become vertical and no increase in $\frac{\dot{m}\sqrt{T_{01}}}{P_{01}}$ can be achieved at these lower pressure ratios.

The Flownex® model's compressor is already set up with the K31 compressor maps, from which initial performance results are produced. Following that, the new impeller design's compressor maps are imported into the Flownex® model to produce new results that are used to evaluate the engine's overall performance improvement.

3. Centrifugal Compressor Design

According to the previously mentioned design methodology, the geometry of the existing centrifugal compressor impeller is measured and replicated in a three-dimensional (3D) modelling tool. This reverse engineering technique is used to provide a baseline design for testing and future improvements. Following that, a one-dimensional (1D) mean line code is applied to iteratively develop a new impeller design based on desired running points.

3.1. Current Impeller

The current K31 compressor consists of an impeller and a vaneless diffuser, which means that the diffuser is simply an open passageway. The basic dimensions of the impeller, such as diameters and axial lengths, are measured manually with a vernier calliper. The remainder of the impeller's dimensions, particularly the blade profiles, have a very complex geometry that necessitates a more sophisticated 3D measuring technique.

The geometry of the impeller, including the complex blade profiles, is captured using a structured light 3D scan method. It works by projecting light in a grid pattern, which becomes distorted when reflected off an object, and cameras catch the reflections to form the model. The EinScan Pro 2X 3D scanner, developed by [8], is used to carry out this task. This device used is housed and administered by [9], located in the Stellenbosch University library. Fig. 5 exhibits the 3D scanner scanning the impeller.

Fig. 5. EinScan Pro 2X 3D scanner

The turntable, on which the impeller is mounted, turns in small increments as cameras record its geometry. The computer program, interacting with the scanner, builds a point cloud of millions of points resembling the impeller. The point cloud is then refined into a solid mesh that replicates the impeller's geometry. From this mesh, exact x, y, and z coordinate point measurements can be captured along all the blade profiles and imported into a 3D modelling program such as Autodesk Inventor® Professional where the blade geometries can be built. Fig. 6 shows the existing K31 impeller alongside the 3D scanned impeller.

(a) **(b)**

Fig. 6. (a) K31 impeller and (b) scanned impeller result

The Einscan Pro 2X claims to deliver a scan accuracy of 0.04 mm, which was validated and proven to be within range. This was accomplished by comparing the basic dimensions of the physical measurements to the same dimensions in the Inventor® 3D model.

3.2. New Impeller and Diffuser Design

The 1D mean-line code is based on a centrifugal compressor design procedure developed by [10]. It has been optimised further, providing users with more control over designing a compressor based on design specifications. It is currently used to assist in the design of centrifugal compressor components such as the impeller and diffuser, and it additionally provides the required geometry file to conduct a computational fluid dynamic (CFD) analysis. A user-friendly graphical user interface (GUI) application (App) in Matlab® for the 1D mean-line code was developed by [11] for assisting users with initial compressor designs. The 1D App follows a logical procedure featuring user inputs and is divided into five steps according to [11], which are listed below:

- Inlet Thermodynamic Conditions: Here, the atmospheric conditions and the fluid characteristics of air are set.
- Impeller Design: The impeller's geometrical inputs are specified at a desired operating speed and output performance. The two-dimensional (2D) blade profile can also be modified, and calculated preliminary performance results can be compared to the intended performance.
- Diffuser Design: Similar to the Impeller Design, geometrical inputs are specified to achieve a desired output performance. The 2D blade profile can be modified, and preliminary performance results are calculated.
- Overall Performance Results: The performance of the impeller and diffuser is calculated at specified operating points, enabling users to validate their initial design.
- CFD Output: The geometry of the impeller and diffuser is exported as a .geomTurbo file, which specifies the blade profiles and operating points. The .geomTurbo file is imported into Numeca FINE™/Turbo software for CFD analysis.

These five steps are performed in an iterative procedure where more than one compressor is designed. CFD simulations provide more accurate results that must be compared and validated to determine the optimal design. The chosen impeller and diffuser generated by the 1D App from the preceding five steps are shown in Fig. 7 below.

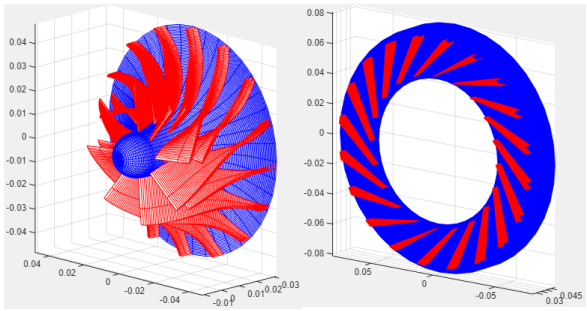

(a) (b)

Fig. 7. (a) Impeller and (b) diffuser 1D App design

The characteristics of this final design were chosen to perform at a higher pressure ratio and efficiency. To aid in this, the tolerance of the gaps between the impeller and its housing is increased to the highest manufacturing tolerance achievable with standard machinery. As a result, the new design's housing gap was decreased from the K31 impeller's 0.65 mm to 0.3 mm. The new impeller design includes an additional main and splitter blade to help reduce a blade loading parameter. In comparison to the vaneless diffuser in the K31 compressor, the new compressor design has a 20-blade vaned diffuser to improve the pressure ratio even higher.

The new design aims to increase the output power of the micro gas turbine (MGT) while improving overall engine efficiency. It intends to achieve this by running the compressor at an ideal operating point based on the compressor maps illustrated from Fig. 4.

4. CFD Analysis

A computational fluid dynamic (CFD) simulation is essential because it gives valuable data that aids in understanding the compressor's performance. It provides the total-to-total pressure ratio and efficiency performance curves that the Flownex® model requires. The CFD software used in this study is Numeca FINE™/Turbo v16.1, which is ideally suited for turbomachinery and functions well with the one-dimensional (1D) application (App).

4.1. Setup

The Reynolds-Averaged Navier-Stokes (RANS) Equations are solved using the Spalart-Allmaras turbulence model in this CFD simulation. In comparison to the two equation models, $k-\varepsilon$ and $k-\omega$, Spalart-Allmaras, a one equation model developed by [12], is chosen for its improved boundary layer prediction in the presence of adverse pressure gradients. Its initial intended use for aerofoil applications has resulted in its popularity for modelling turbomachinery applications.

The CFD simulation requires a mesh configuration, which entails dividing the domain into a grid. Before the three-dimensional (3D) mesh is generated, the grid pattern and number of points along the blades are adjusted in a two-dimensional (2D) blade-to-blade (B2B) mesh. This process is necessary to ensure that the grid achieves a good quality, where its orthogonality, aspect ratio, and expansion ratio are all within a particular range. Table 1 lists the recommended requirements for these in accordance with [13], along with the worst results and the percentage of these "bad cells" that were obtained.

Table 1. Mesh quality results

Quantity	Criteria	Worst Value	% Bad Cells
Orthogonality	> 25°	22°	0.098%
Aspect ratio	< 2500	519	0%
Expansion ratio	< 1.8	2.4	0.999%

Further quality optimisation steps are performed on the mesh to guarantee that it meets the Spalart-Allmaras criteria for the non-dimensional distance, y^+, at the walls. The y^+ distribution mostly stayed within the required range of 1 to 10, with minimum and maximum values of 0.142 and 11.172 at non-critical locations. The size of the grid cells is checked for mesh independence, where the results of a coarse, medium, and fine mesh are compared. This is accomplished by generating a performance curve from simulations of each of the three meshes at a particular operating speed, as shown in Fig. 8.

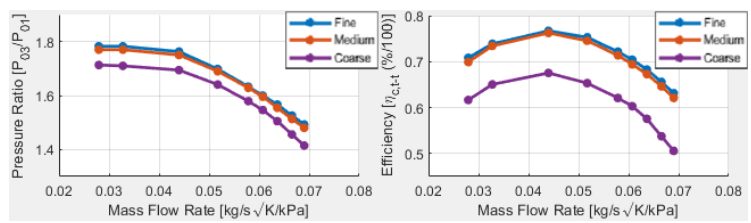

(a) (b)

Fig. 8. (a) Pressure ratio and (b) efficiency mesh independence performance curves

The performance curve produced by the coarse mesh differed from the curves generated by the medium and fine meshes. Whereas the performance curves generated by the medium and fine meshes were almost exact. Therefore, mesh independence is achieved because any further increase in mesh density will not significantly improve the results.

The remainder of the CFD setup entails establishing the domain and its boundary conditions, as well as setting the necessary output variables to be analysed. The inlet, outlet, periodic, and solid boundaries make up the domain's boundary conditions. The inlet and outlet boundaries denote the locations where air flows into and out of the domain. The inlet boundary is set up to replicate atmospheric air conditions of 100 000 Pa and 298 K, while the outlet boundary is defined as a mass flow imposed,

which specifies a particular mass flow rate for the simulation to run at. Finally, the solution's convergence is monitored and approved when the inlet and outlet mass flow rates are equal. It is limited to a maximum of 6 000 iterations, giving the solution sufficient time to converge and meet this condition.

4.2. CFD Results

The CFD simulations are used to generate the compressor maps, as shown in Fig. 4, which are required by the Flownex® model. This is done by simulating various mass flow rate points along the operating range, and then assessing the results to calculate the pressure ratio and efficiency from Eq. (1) and Eq. (2) respectively. Lowering the mass flow rate until the pressure ratio reaches a maximum value determines the stall point, or lower mass flow rate boundary. The choke point, or upper mass flow rate boundary, is defined as the point where the pressure ratio curve becomes vertical and no further increase in mass flow rate is possible. The choke point is found by specifying an unrealistically low outlet pressure and then running the simulation to determine the choke mass flow rate. These curves are constructed at various operating speeds to collect adequate data for the Flownex® model.

To begin, the scanned replica impeller is simulated in CFD to obtain its compressor maps, which are then compared to those of the K31 to validate the CFD accuracy. These curves are shown in Fig. 9 below, with the scanned replica impeller's curves superimposed on the K31 curves.

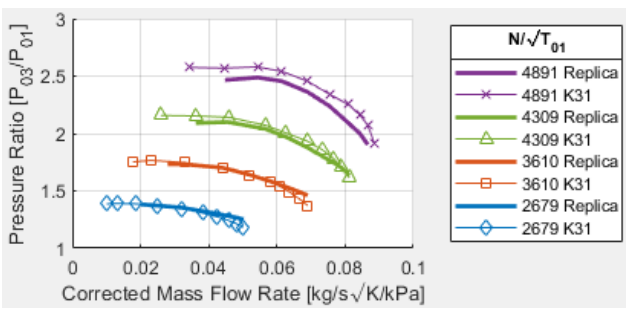

(a)

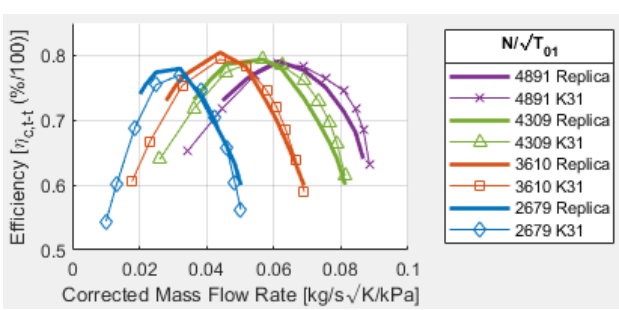

(b)

Fig. 9. (a) Pressure ratio and (b) efficiency compressor maps of scanned replica and K31 impeller

The curves of the scanned replica mostly match those of the K31, with maximum deviations of 6.5% and 6.8% for the pressure ratio and efficiency, respectively. It is concluded that a minor deviation is to be expected because the K31 maps are obtained from actual test runs where more losses are present. Because actual test runs on the compressor allow for pushing further boundary points than a CFD simulation can produce, the stall point of the K31 maps occurs further to the left, as expected.

The new designed impeller and diffuser were subject to the same CFD simulation conditions and method of constructing the performance curves. The compressor map curves of the new design are compared to those of the scanned replica in Fig. 10.

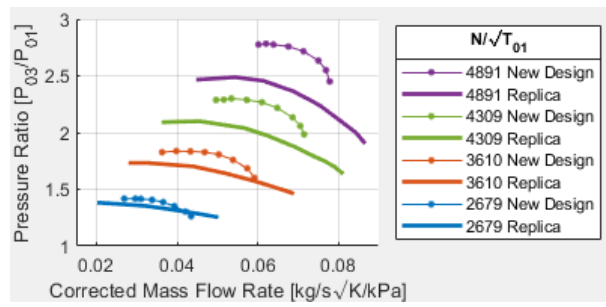

(a)

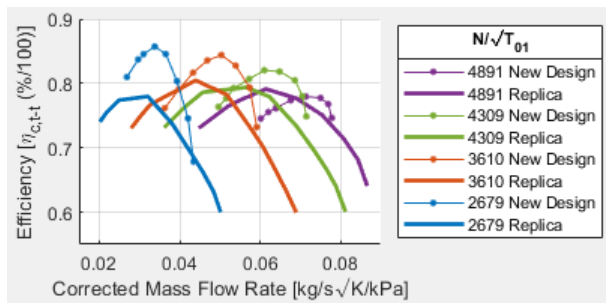

(b)

Fig. 10. (a) Pressure ratio and (b) efficiency compressor maps of new design and scanned replica impeller

The new design displays a narrower operating range compared to the replica due to one additional impeller main and splitter blade and the addition of the vaned diffuser, causing choking to occur earlier. However, it produces a higher pressure ratio and efficiency at each of the engine speeds' optimal operating point, indicating that it can provide better performance for the micro gas turbine (MGT).

5. Results

The K31 compressor maps are first configured to the compressor in the Flownex® model, and the MGT is simulated to obtain initial results. The compressor maps of the scanned replica impeller are then configured to the compressor of the Flownex® model to verify how closely they match. Subsequently, the

compressor maps of the Flownex® model are replaced with maps of the new compressor design to determine the improvements in performance. A constant engine speed of 53 000 rpm is chosen because this is the observed speed at which all the compressors run at peak efficiency. The compressor and overall operating performance results of the Flownex® model are listed in Table 2.

Table 2. Flownex® model MGT results

	$PR_{C(tt)}$ [-]	$\eta_{C(tt)}$ [%]	$\dot{m}_C$ [kg/s]	$\dot{W}_{out}$ [kW]	η_{MGT} [%]
K31	1.477	77.8	0.218	17.8	8.86
Replica	1.482	78.3	0.219	18.078	8.93
New design	1.55	84.2	0.241	22.186	9.96

The replica's design results match the operating point of the K31 compressor with a minor variance, resulting in a total output power that is 1.56% higher. This was expected given that the scanned replica impeller's compressor maps are based on a CFD simulation executed under ideal conditions, whereas the K31's are based on actual test runs. The compressor results of the new design enhance the pressure ratio and efficiency operating points, boosting the MGT engine output power by 22.7% above the scanned replica's performance.

6. Discussion and conclusion

This paper presents the redesign of a centrifugal compressor for an MGT engine used for a solar-hybrid application. A Flownex® model of this MGT is examined where its performance can be predicted, and its compressor stage is defined by compression performance charts. The geometry of the existing impeller is replicated in software, which was done by a 3D scanner. The 1D App was used to aid in the development of a new impeller and diffuser design. CFD simulations are performed on both the scanned replica and the new design to generate performance charts for further modelling the MGT's performance in the Flownex® model.

The compressor maps of the scanned replica exhibited a small variance when compared to the K31 compressor maps. The MGT's overall output power deviates from 17.8 kW, when configured with the K31 maps, to 18.078 kW, when configured with the scanned replica's maps. Modelling the new design's compressor maps yield a substantially higher compressor operating point at which the engine's power improves by 22.7% from 18.078 kW, of the scanned replica impeller, to 22.186 kW.

This modification to the MGT improves overall performance by enabling the MGT's compression stage to offer an optimal operating point. The new compressor not only boosts the output power of the solar-hybrid MGT configuration, but it also allows for future modifications in other stages of the engine to extract the maximum performance achievable from this system.

Acknowledgements

This project was partially funded by the National Research Foundation (NRF) of South Africa (Grant Number 141891).

References

[1] SolarGIS, 2020. Direct Normal Irradiance (DNI). [Online] Available at: https://solargis.com/maps-and-gis-data/download/south-africa [Accessed 19 April 2022]

[2] Kröger, D., 2011. The Stellenbosch University Solar Power Thermodynamic cycle. [Online] Available at: https://sterg.sun.ac.za/wp-content/uploads/2011/05/SUNSPOT-2.pdf [Accessed 19 April 2022].

[3] Ssebabi, B., 2020. Development of a Micro Gas Turbine for Central Receiver Concentrating Solar Power Systems, Stellenbosch: PhD, Stellenbosch University.

[4] Hummel, S., 2014. Berechnung und Konstruktion einer Brennkammer für eine Mikrogasturbine, s.l.: Final year project, University of Stuttgart.

[5] Saravanamuttoo, H., Cohen, H. & GFC, R., 2009. Gas Turbine Theory. 5th ed. s.l.:Pearson Education

[6] Dixon, S. & Hall, C., 2010. Fluid Mechanics and Thermodynamics of Turbomachinery. 6th ed. s.l.:s.n.

[7] Afeltra, M., 2022. The Development of a Recuperator for a Solar Hybrid Micro Gas Turbine System, Stellenbosch: Masters, Stellenbosch University.

[8] 3D, S., 2023. About SHINING 3D. [Online] Available at: https://www.shining3d.com/about-us/ [Accessed 30 March 2023].

[9] Service, S. L. a. I., 2023. Makerspace: 3D Scanning. [Online] Available at: https://libguides.sun.ac.za/makerspace [Accessed 30 March 2023].

[10] Aungier, R., 2000. Centrifugal Compressors, New York: ASME Press.

[11] Van Eck, H., 2020. Development of a One-Dimensional Code for the Initial Design of a Micro Gas Turbine Compressor Stage, Stellenbosch: Masters, Stellenbosch University.

[12] Spalart, P. R. & Allmaras, S. R., 1994. A one-equation turbulence model for aerodynaic flows, s.l.: s.n.

[13] De Villiers, L., 2013. Numeca Manual for the Design of a Centrifugal Compressor, s.l.: Stellenbosch University.